IOP Publishing Measurement Science and Technology

Meas. Sci. Technol. **31** (2020) 054009 (6pp) https://doi.org/10.1088/1361-6501/ab6b50

A reference-scan-based method for correcting the nonlinear drift of atomic force microscopy at sub-nanometer precision

Ryosuke Kizu, Ichiko Misumi, Akiko Hirai and Satoshi Gonda

National Metrology Institute of Japan (NMIJ), National Institute of Advanced Industrial Science and Technology (AIST), Tsukuba, Ibaraki 305-8563, Japan

E-mail: r-kizu@aist.go.jp

Received 22 November 2019, revised 5 January 2020
Accepted for publication 14 January 2020
Published 5 March 2020

Abstract

A known fundamental issue with atomic force microscopy (AFM) is that drift occurs during an AFM measurement, distorting the AFM image. In this study, a method for correcting this nonlinear drift in two dimensions (the vertical axis and one of the two horizontal axes) is proposed and demonstrated. A normal AFM measurement is accomplished with many fast-scan profiles, using the raster scan method. In the proposed drift-correction method, the first-scanned profile is set as the reference profile, and the scan at the first-scanned location is inserted periodically during the normal profile scans. The normal scanned profiles are used to construct a normal AFM image, which is distorted by the drift. The time-dependent drift distance can be estimated by a series of the scanned reference profiles, and the distorted AFM image is corrected using this estimated distance. It is shown, experimentally, that the drift correction in two dimensions has both high resolution and repeatability at the sub-nanometer scale.

Keywords: drift correction, atomic force microscopy (AFM), dimensional nanometrology

(Some figures may appear in colour only in the online journal)

1. Introduction

Dimensional nanometrology is the most basic function of atomic force microscopy (AFM) [1]. Highly accurate, precise nanometrology by AFM is important for nanoscale calibration standards used in the semiconductor industry and precision engineering; it is even more important for next-generation devices and material development. The 3D shape of the nanoscale line pattern fabricated on a semiconductor wafer is evaluated using many different parameters, such as height, critical dimension (CD, e.g. linewidth), surface roughness, line edge roughness (LER), line width roughness (LWR), and sidewall angle [2]. In the semiconductor industry, metrological demands on these parameters have now reached sub-nanometer precision, and such measurement accuracy should be ensured using nanoscale calibration standards [3].

If an AFM image is distorted, then the nanoscale structures' dimensional parameters extracted from that image will contain errors. Fluctuation in the position of the AFM probe relative to the sample during measurement, known as drift, distorts the AFM image. One of the main causes of such drift is shrinkage or expansion of the microscope's components due to thermal variation [4]. The drift is nonlinear and difficult to correct. A simple drift correction assumes a constant drift rate; in such cases, the effect of the nonlinearity of the drift remains as a correction error. Recent high-end commercial AFM instruments reduce the drift by stabilizing the measurement environment and using materials with low thermal expansion for the instrument's components. However, there is a limit to how far these approaches can reduce the drift. Moreover, a low scanning speed is necessary considering the scanner control stability and tip wear for accurate dimensional measurement. That is, an AFM image is a result of the sample shape, the drift distortion effect, and the tip shape (known as tip convolution). It is impossible to correct the variation in tip convolution caused by the tip wear during the measurement. Thus, to suppress the tip wear, an AFM measurement often takes a few tens of minutes or more. In such situations, the drift must be corrected with sub-nanometer precision, including the effect of the nonlinearity of the drift.

There is a hardware-based drift-correction method that involves using an interferometer and monitoring the distance between the AFM probe and the sample with a small 'measurement loop' [5–8]. There are also several software-based drift-correction methods that avoid the need to modify instruments. These software-based methods with relatively high precision, classified as methods 1–3, are as follows. (1) The drift rate is estimated from multiple images that are measured repeatedly from the same area and compared to calculate the drift rate [9]. (2) The AFM image distortion is corrected using an ancillary AFM image that is measured after the main AFM image. The ancillary image is a narrow, rectangular image whose fast-scan axis is the same as the slow-scan axis of the main image [4, 10]. The ancillary AFM image, regarded as having no drift because of its short measurement time, is used as the reference image of the main AFM image. (3) The height drift is corrected using self-intersecting scan paths to distinguish the drift from the surface topography. Observing the height differences when passing the same position at different times enables reconstruction of a continuous function for the drift [11].

However, the aforementioned software-based methods have the following weaknesses. Method 1 cannot correct the nonlinear drift distortion that occurs during a single AFM measurement because its time resolution is the time that it takes to complete a single AFM measurement. Method 2 causes errors because of the low matching precision. The ancillary AFM image must be measured within a short time, so as not to be affected by drift; therefore, it contains small number of profiles. The result is a low degree of matching with the main AFM image, and the correction precision is insufficient for sub-nanometer precision. Method 3 causes errors because of the low matching precision as it cannot correct the horizontal drift with sub-nanometer precision. Additionally, with methods 2 and 3, the same xy-position is measured multiple times from different directions, and that causes variation in the z-values. That is because different scanning directions give rise to different tip convolutions in the scanned profiles because of (i) the cone-shaped tip geometry's asymmetry, (ii) the imperfect parameter setting (PID parameters of closed-loop control, AFM set point, and scan speed), and (iii) the electrical and mechanical noise of the actual AFM instrument. To date, no method for correcting the nonlinear drift has been demonstrated experimentally with sub-nanometer resolution and repeatability.

In this paper, we propose and demonstrate a reference-scan-based method for correcting the nonlinear drift in two dimensions (namely the height and fast-scan axes). The method involves measuring the nonlinear drift that occurs during a single AFM measurement of a nanoscale line pattern with high time and spatial resolutions. The repeatability is evaluated by comparing the results that were measured repeatedly at the same position.

2. Method of drift correction and experimental setup

2.1. Method

An AFM image is generally taken by raster scan; namely, it is obtained by a fast scan that takes line profiles of the sample and a slow scan in which the AFM tip moves repeatedly by a small distance in a direction orthogonal to the fast-scan axis, alternating with a fast scan. Therefore, the AFM image is formed from many fast-scan profiles. The drift correction proposed in this study is a reference-scan-based method, in which a scan of one reference profile is measured periodically to obtain the drift distances. The first fast-scan profile is set as the reference profile ($\boldsymbol{P}_1 = \boldsymbol{P}_{\mathrm{ref}}$, which is an array of sampled points in the scan). Then, the reference profile is scanned repeatedly, at regular intervals, during the normal AFM measurement, where the normal AFM image is distorted by the drift. For example, scans for the normal AFM measurement and the reference profile are conducted alternately, as shown in figure 1. In data processing, after the measurement, even-numbered profiles $\boldsymbol{P}_{2n}$ ($n = 1, 2, \ldots$) (reference profiles measured at different times) and $\boldsymbol{P}_{\mathrm{ref}}$ are compared, then the two-dimensional deviation (along the height and fast-scan axes) is calculated for each $\boldsymbol{P}_{2n}$, as shown in figure 2. The matching algorism is basically same as 2D iterative closest point (ICP) algorism, which is simpler than 3D ICP algorism used in the reference [12]. The deviation in two directions represents a drift distance $\boldsymbol{d}_{2n} = (y_{2n}, z_{2n})$ from the initial tip position (when the AFM measurement was started) to the tip position at $2n$-th scan. That is, the time-dependent drift distance in the two directions is found with a time resolution of the period of the reference-profile measurements. The final AFM image is constructed from only the odd-numbered profiles $\boldsymbol{P}_{2n-1}$ ($n = 1, 2, \ldots$) with correction of the drift by interpolating $\boldsymbol{d}_{2n-2}$ and $\boldsymbol{d}_{2n}$.

The proposed method does not correct the drift along the slow-scan direction. There are two requirements for applying the drift correction. One is that the slow-scan axis (horizontal) drift rate should be small enough, considering the total measurement time. On one hand, the horizontal drift is often smaller than the height drift in the stabilized environment because of the horizontally symmetric construction of the AFM instrument [4]. Conversely, constructing a vertically symmetrical AFM instrument is difficult; thus, the vertical drift becomes larger than the horizontal drift. Therefore, several previous studies were aimed at correcting the vertical drift [4, 5, 11]. The other requirement is that the cross section around the reference profile should be uniform within the area of supposed drift, during the measurement, along the slow-scan axis. This is because the calculated $\boldsymbol{d}_{2n}$ has an error if the $\boldsymbol{P}_{\mathrm{ref}}$ shape is changed during the measurement because of the drift along the slow-scan axis, and the $\boldsymbol{P}_{\mathrm{ref}}$ shape should be constant even if drift occurs along the slow-scan axis. As illustrated in figure 1,

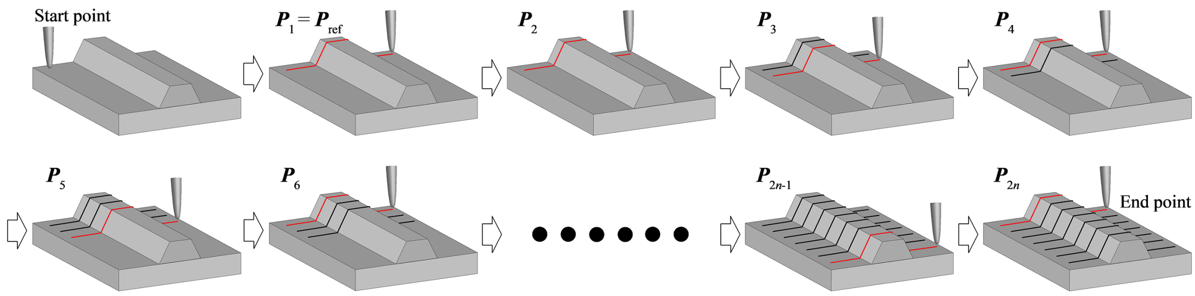

Figure 1. Reference-scan-based method for correcting nonlinear drift. The scans of the normal AFM measurement and the reference profile are conducted alternately.

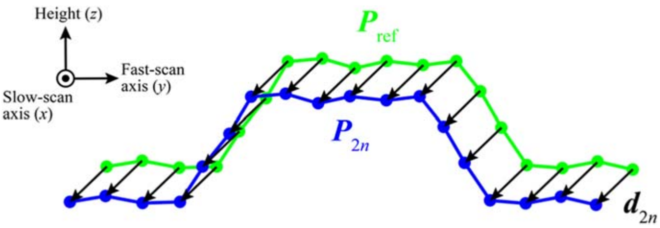

Figure 2. Drift distance $\boldsymbol{d}_{2n}$ is calculated so that $\boldsymbol{P}_{2n}$ and $\boldsymbol{P}_{\text{ref}}$ are best matched. $\boldsymbol{d}_{2n}$ has two dimensions (namely the height and fast-scan directions).

a line pattern is one of the patterns that satisfy the above requirements.

2.2. Experiment

We demonstrated the proposed method by measuring a trapezoidal line pattern (AS200P-A, NTT Advanced Technology Corp.; the height and top width are approximately 170 nm and 400 nm, respectively) using a metrological AFM developed by the National Metrology Institute of Japan [13]. The trapezoid line pattern was formed by anisotropic etching of a Si(100) substrate and had a taper angle of 54.7°. The AFM probe used in the measurement was an OMCL-200TS (resonance frequency: 150 kHz (typ.); spring constant: 9 N m^{-1} (typ.); Olympus Corp.). The measurement range was 900 nm (*x*: slow axis, longitudinal direction of line pattern) × 900 nm (*y*: fast axis, linewidth direction) with 600 lines × 600 points. The measurement time was approximately 50 min. Note that the measurement time was twice that of a normal AFM measurement because of the scans of $\boldsymbol{P}_{2n}$ for the drift calculation. Five measurements were repeated at the same position to verify the drift-correction repeatability.

3. Results and discussion

3.1. Calculation and correction of drift from measured AFM data

Figures 3(a) and (b) show the measured image, expressed as surface rendered and 3D point cloud, respectively. The top part of the trapezoidal line pattern is enlarged in figure 3(c) to show the drift distortion. There are $\boldsymbol{P}_{2n}$ (blue) data at the same *x*-position (slow-scan axis) of $\boldsymbol{P}_{\text{ref}}$ (green). The $\boldsymbol{P}_{2n}$ data go downward along the *z*-axis from the beginning position of $\boldsymbol{P}_{\text{ref}}$; therefore, the drift direction in the *z*-axis was downward. The $\boldsymbol{P}_{2n-1}$ (red) data are used to construct the AFM image that is distorted by the drift and not yet corrected. $\boldsymbol{P}_{2n}$ was compared to $\boldsymbol{P}_{\text{ref}}$ and translated by $\boldsymbol{d}_{2n}$ in two directions (the *y*- and *z*-axes) so that each $\boldsymbol{P}_{2n}$ best matched with $\boldsymbol{P}_{\text{ref}}$. Figure 4(a) shows $\boldsymbol{d}_{2n}$ with respect to the profile numbers for the two directions (*y*- and *z*-axes), and figure 4(b) shows the top part of the AFM image before and after the correction.

3.2. Resolution and repeatability of drift correction

Five measurements were repeated at the same position to verify the drift-correction repeatability, with the top part of the trapezoidal line pattern being compared for the five results. Figures 5(a) and (b) show $\boldsymbol{d}_{2n}$ in the *y*- and *z*-axes, respectively, and the horizontal axis also corresponds to the slow-scan axis (*x*-axis). Figures 5(c) and (e) show the sidewall part of the five results in the range of $-81.5 \text{ nm} \leq z \leq -78.5$ nm before and after the drift correction is applied using $\boldsymbol{d}_{2n}$, respectively. These are projected onto the *xy*-plane to confirm the effect of the correction in the *y*-axis. Here, to show the degree of agreement of five results, the *y*-offset of the profiles at the position $x = -450$ nm are aligned. The difference of offsets, which were adjusted in figures 5(c)–(f), was caused by tip wear during measurement, which results in linewidth increase. Note the projected profile looks quantized because the sampling step on the *y*-axis was 1.5 nm. Figures 5(d) and (f) show the top part of the five results in the range of $-1.5 \text{ nm} \leq y \leq 1.5$ nm before and after that the drift correction is applied using $\boldsymbol{d}_{2n}$, respectively, that are projected onto the *xz*-plane to confirm the effect of the correction in the *z*-axis. Figure 6 shows linewidth variation along *x*-axis at the half height. Table 1 shows the average linewidths along *x*-axis for 900 nm and the differences of linewidth from preceding result.

3.3. Discussion

Figure 4(a) shows that the drift, nonlinearly changed in both the *y*- and *z*-axes, during the AFM measurement. Because of the proposed method, the drift distance was obtained with a time resolution of the period of the reference-profile measurements and with sub-nanometer resolution, which corresponds roughly to the noise level in the smoothly changed drift

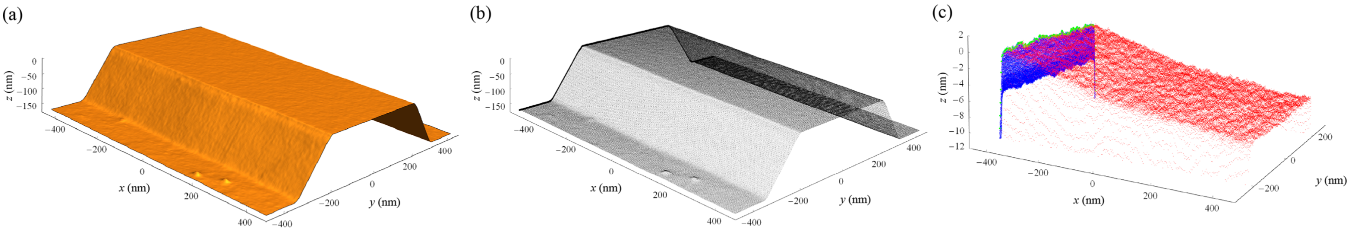

Figure 3. (a) Surface rendered and (b) 3D point cloud AFM image of trapezoid line pattern using the proposed scan method. (c) Top part of (b) enlarged to show the drift distortion. The $\boldsymbol{P}_{2n}$ (blue) data are used to calculate the drift, and the $\boldsymbol{P}_{\mathrm{ref}}$ (green) and $\boldsymbol{P}_{2n-1}$ (red) data form the AFM image, which is distorted by the drift.

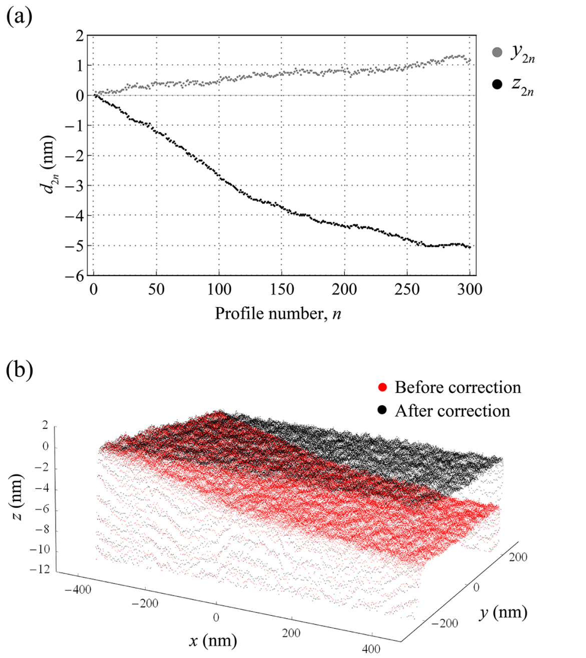

Figure 4. (a) Drift distance $\boldsymbol{d}_{2n} = (y_{2n}, z_{2n})$ with respect to profile number for two directions (y- and z-axes). (b) Top part of the AFM image before (red) and after (black) correction using $\boldsymbol{d}_{2n}$.

distance. Therefore, the distorted AFM image was corrected by the obtained drift distance figure 4(b). The total drift distances along the y- and z-axes were 1.2 nm and 5.0 nm, respectively, and the total measurement time was 50 min, thus the average drift rates along the y- and z-axes were 0.02 nm min^{-1} and 0.1 nm min^{-1}, respectively.

In figures 5(c) and (d), the five results before the drift correction became dispersed as profile number become larger along both the y- and z-axes. This shows the nonlinear drift occurred in the AFM measurements. The five results after the drift correction, corrected with $\boldsymbol{d}_{2n}$ figures 5(a) and (b), are well matched in figures 5(e) and (f). In particular, the difference between the corrected five results of figure 5(f) is less than 1 nm over the entire range of the x-axis. This shows that the proposed drift correction is highly repeatable at the sub-nanometer scale even when nonlinear drift occurs. Compared to methods 1–3, discussed in section 1, the proposed method can correct the nonlinear drift, in contrast to method 1, and is more accurate than methods 2 and 3 because the tip-convolution effect is canceled. The tip scan directions of $\boldsymbol{P}_{2n}$ and $\boldsymbol{P}_{\mathrm{ref}}$ are the same in the proposed method, unlike in methods 2 and 3.

The slight errors in the five corrected results, seen in figures 5(e) and (f), were caused by (i) the calculation error of matching $\boldsymbol{P}_{2n}$ with $\boldsymbol{P}_{\mathrm{ref}}$, (ii) AFM measurement noise, (iii) the tip-position error caused by the drift in the slow-scan direction, and (iv) tip wear during measurement. Although the tip-position error is less than few nanometers, the fast-scan profiles differ regarding sub-nanometer precision because the local surface roughness on the line pattern fluctuates on the sub-nanometer scale. There is a possibility that tip wear alters tip-convolution effect and leads correction error in y-direction. The z-axis drift correction figures 5(b), (d), and (f) is not affected by tip wear, because tip convolution has no influence on one-directional probing such as step height measurement [14]. Moreover, it is corrected simultaneously as z-axis drift in a way that they are indistinguishable. On the other hand, y-axis drift correction figures 5(a), (c), and (e) may be affected by tip wear, because it is bi-directional probing and the tip convolution changes due to the tip wear. In this study, the tip scanning speed was carefully adjusted to minimize tip wear. The averaged tip wear per one measurement was 1.3 nm from table 1, therefore the expansion per one sidewall of the trapezoid line pattern was 0.7 nm. Such a small tip wear made small error and corrected five results were well matched each other. However, large tip wear would make non-negligible error, thus prevention of tip wear such as slow scan speed or use of high durable material tip (e.g. diamond like carbon) is important.

The drift correction proposed in this study has a limitation related to an applicable sample. When there is drift along the slow-scan axis, the reference profiles at different times are different; thus, the calculated drift distance may have errors. The proposed method is suitable for nanoscale line patterns because the shape variation along the slow-scan axis is moderate. Such patterns are used to calibrate nanoscale standards, where highly accurate measurement is required. The error in the proposed method is sufficiently small and has negligible influence on the dimensional parameters of the line pattern, such as height, linewidth, and LER/LWR [12–17].

As a future work, drift correction is also required in the slow-scan direction. For example, a reference profile, and several profiles around the reference profile, could be measured as a reference-profile set. Next, each profile measured for the drift calculation could be compared to each member of the reference-profile set. The drift distance along the slow-scan axis is the difference of the values of slow-scan

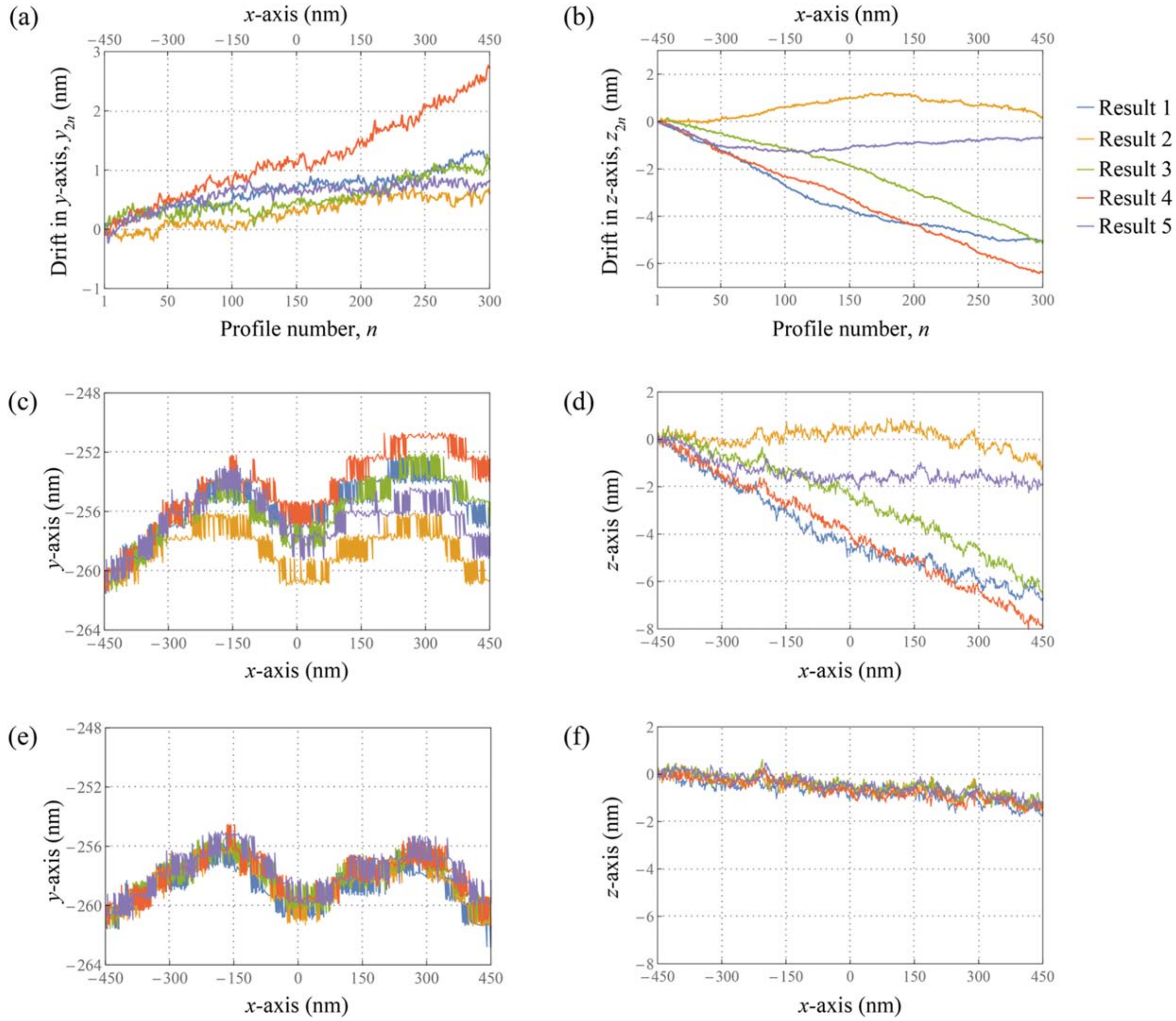

Figure 5. Drift distance $\boldsymbol{d}_{2n}$ of five results with respect to profile numbers in (a) y-axis and (b) z-axis. The sidewall part of the five results in the range of -81.5 nm $\leq z \leq -78.5$ nm is projected onto xy-plane (c) before and (e) after that the drift correction was applied. The top part of the five results in the range of -1.5 nm $\leq y \leq 1.5$ nm is projected onto xz-plane (d) before and (f) after that the drift correction was applied.

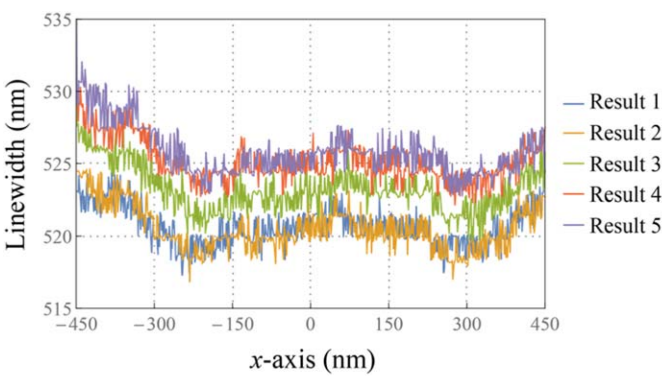

Figure 6. Linewidth variation along x-axis.

Table 1. The average linewidths at the half height and the expansions of linewidth of the five results.

Result No.	Average linewidth (nm)	Difference from the preceding result (nm)
1	520.7	–
2	520.5	−0.2
3	523.3	2.8
4	525.2	1.9
5	525.8	0.7

axis of the most-matched profile and the first reference profile. Finally, the drift along the z-axis and the fast-scan axis could be calculated in the same manner as in figure 2; thus, the drift along three axes would be found.

4. Conclusions

A reference-scan-based method for correcting the nonlinear drift of an AFM image was proposed and experimentally demonstrated. The method involves a scan of one reference profile being measured periodically during the AFM measurement to obtain each drift distance each time the reference profile is measured. The results show the proposed method offers sub-nanometer resolution along two axes (the height and fast-scan axes). The drift correction was repeated five times at the same position, and the results showed it is highly repeatable on the sub-nanometer scale. Although the proposed method is limited by requiring a target sample with a uniform cross section along the slow-scan axis, it has the highest resolution and repeatability among drift-correction methods and is beneficial for calibrating nanoscale standards.

Acknowledgments

This work was supported by JSPS KAKENHI Grant No. JP16K18119.

ORCID iDs

Ryosuke Kizu https://orcid.org/0000-0002-9638-0006
Ichiko Misumi https://orcid.org/0000-0001-5431-7298
Akiko Hirai https://orcid.org/0000-0003-0198-8922
Satoshi Gonda https://orcid.org/0000-0003-4535-1878

References

[1] Binnig G, Quate C F and Gerber C 1986 Atomic force microscope *Phys. Rev. Lett.* **56** 930–3
[2] Bunday B, Solecky E, Vaid A, Bello A F and Dai X 2017 Metrology capabilities and needs for 7nm and 5nm logic nodes *Proc. SPIE* **10145** 10145G
[3] Yacoot A and Koenders L 2011 Recent developments in dimensional nanometrology using AFMs *Meas. Sci. Technol.* **22** 122001
[4] Marinello F, Bariani P, Chiffre L D and Savio E 2007 Fast technique for AFM vertical drift compensation *Meas. Sci. Technol.* **18** 689–96
[5] Sikora A, Sokolov D V and Danzebrink H U 2005 Scanning probe microscope setup with interferometric drift compensation *Nanoscale Calibration Standards and Methods* ed G Wilkening and L Koenders (Weinheim: Wiley-VCH) pp 109–18
[6] Yacoot A, Koenders L and Wolff H 2007 An atomic force microscope for the study of the effects of tip–sample interactions on dimensional metrology *Meas. Sci. Technol.* **18** 350–9
[7] Ducourtieux S and Poyet B 2011 Development of a metrological atomic force microscope with minimized Abbe error and differential interferometer-based real-time position control *Meas. Sci. Technol.* **22** 094010
[8] Meli F 2011 New traceable atomic force microscope for dimensional measurements *METinfo* **18** 4–9
[9] Clifford C A and Seah M P 2009 Simplified drift characterization in scanning probe microscopes using a simple two-point method *Meas. Sci. Technol.* **20** 095103
[10] Salmons B S, Katz D R and Trawick M L 2010 Correction of distortion due to thermal drift in scanning probe microscopy *Ultramicroscopy* **110** 339–49
[11] Meyer T R *et al* 2014 Height drift correction in non-raster atomic force microscopy *Ultramicroscopy* **137** 48–54
[12] Kizu R, Misumi I, Hirai A, Kinoshita K and Gonda S 2019 Linewidth calibration using a metrological atomic force with tip-tilting mechanism *Meas. Sci. Technol.* **30** 015004
[13] Kizu R, Misumi I, Hirai A, Kinoshita K and Gonda S 2018 Development of a metrological atomic force with tip-tilting mechanism for 3D nanometrology *Meas. Sci. Technol.* **29** 075005
[14] Dai G, Halm K, Bosse H and Dixson R G 2017 Comparison of line width calibration using critical dimension atomic force microscopes between PTB and NIST *Meas. Sci. Technol.* **28** 065010
[15] Haycocks J and Jackson K 2005 Traceable calibration of transfer standards for scanning probe microscopy *Precis. Eng.* **29** 168–75
[16] Dixson R G, Allen R A, Guthrie W F and Cresswell M W 2005 Traceable calibration of critical-dimension atomic force microscope linewidth measurements with nanometer uncertainty *J. Vac. Sci. Technol. B* **23** 3028–32
[17] Dai G, Haßler-Grohne W, Hüser D, Wolff H, Danzebrink H U, Koenders L and Bosse H 2011 Development of a 3D-AFM for true 3D measurements of nanostructures *Meas. Sci. Technol.* **22** 094009